Global Interpretation and Local Analysis to Measure Gears Eccentricity

Joaquín Salas

CICATA-IPN
salas@ieee.org

Abstract. This paper presents a data-driven approach to profile fitting where global constraints are imposed to local measurements. The local measurements are obtained from partial analysis of the objects under consideration. Prior knowledge of the object under analysis provides global constraints. To illustrate these concepts, it is developed the exercise of measuring a gear's boundary from its teeth profile. A framework is developed to extract local parameters from frame to frame and to enforce morphologic constraints over the whole sequence. It is shown how a combination of accurate local processing techniques and global knowledge can solve the tradeoff between what can be perceived locally and interpreted globally.

1 Introduction

Suppose that one is given the task to obtain the geometric properties of a circular object, *i.e.*, compute a circle's center and radius. A possible approach may be to grab an image, detect its contour and from it approximate both its center and its radius. But say, that now one is willing to challenge the hypothesis about the circularity of the boundary. A possible approach may be to zoom in the object's boundary, to reveal more detail, and grab a sequence of images while the object rotates. Then, the problem becomes to find the set rotations and translations that relate features found among the images. Indeed, as the detail level is increased more frames are needed to represent the periphery. If one proceeds from frame to frame the overall error will increase because each transformation adds up some estimation error that accumulates through the sequence. This paper presents a data-driven approach to profile fitting where global constraints are imposed to local measurements. The local measurements are obtained from partial analysis of the objects under consideration. The global constraints are obtained from knowledge about the objects that we are dealing with. In our case, internal spur gears, *i.e.*, they have teeth that are straight and parallel to the axis of rotation and on the inside of a hollow cylindrical shape.

In a seminal work, David Marr[1] introduced the concept of top-down and bottom-up approaches to computer vision systems. Since then, there has been a considerable interest on the integration of global constraints (see Ullman[2] for a description of high-level vision problems), which are usually associated with shape and spatial relations, and local properties, such as the extraction of certain

A. Sanfeliu et al. (Eds.): CIARP 2004, LNCS 3287, pp. 669–676, 2004.

Fig. 1. Experimental Setup. A gear is placed in front of a camera. Then, the gear is rotated manually very slowly while grabbing snapshots. The gear is standing on a metallic base. This causes considerable friction. Before being used the images are corrected using Zhang[5] camera calibration procedure.

physical properties. In this study, global constraints about a gear's circularity are applied to local measurements about the transformation from frame to frame. First, snapshots are acquired while the gear rotates. Each image has information about a few teeth (see Figs. 1 and 2). The translation from frame to frame is computed by applying an iterative registration procedure to the points in the gear's border. The rotation is computed with a closed form equation. Once, the local measurements are acquired, global coherence is enforced. The periodicity of the gear's teeth is used to correct the error accumulation carried out from frame to frame. Methods to measure a gear's profile may be classified as intrusive or non-intrusive. For instance, intrusive methods include a gauge pin that physically touch the gear's surface and translate the relative displacement into depth measurements[3]. Non-intrusive methods include optical comparators that magnify the object by projecting the shadow on a flat screen [4]. Our approach takes the best of both methods, leading to a non-invasive, high-accuracy system to measure an object's profile.

A central problem that we deal with is registration. Registration is the problem of finding the transformation that leads a data set into another. Because its pervasiveness in domains such as Computer Vision, Pattern Recognition, Medical Image Analysis and Remotely Sensed Data Processing, much effort has been devoted to solve it[6]. Significant progress has been made and nowadays registration is used for images that come from different sensors, viewpoints, times and patterns. Despite the variety of applications and categories, registration usually involves finding the transformation of a two-dimensional image patch. This transformation may be affine, perspective, projective or polynomial. In [7], Maintz and Viegever present an extensive overview of registration methods. In most cases, the registration transformation is usually found by establishing an optimization criterion. Although it has been observed that high dimensional

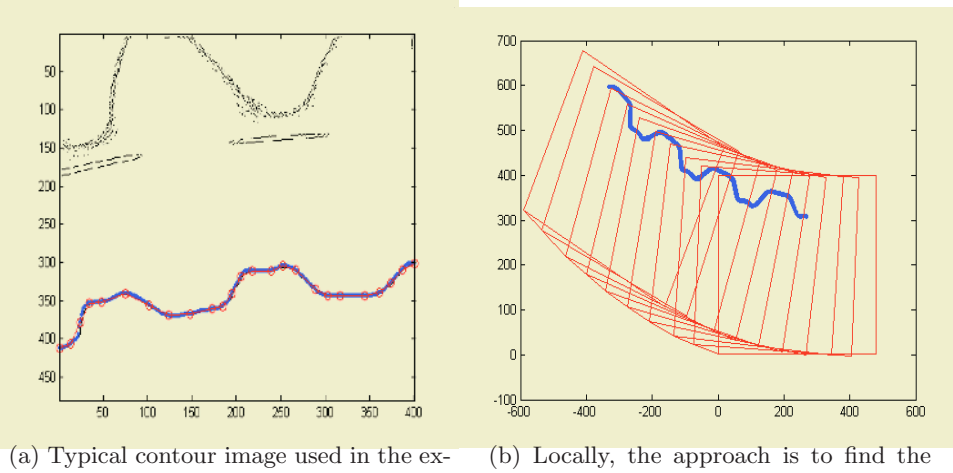

(a) Typical contour image used in the experimentation. It includes the set of profile points and the piecewise approximation with line segments.

(b) Locally, the approach is to find the geometric transformation from frame to frame. Globally, *a priori* knowledge about the object geometry is incorporated into the interpretation.

Fig. 2. Local measurements (a) are integrated by a set of constraints which leads to a global interpretation(b).

transformations involved in deformable registration generally make the problem ill-conditioned [8]. Shi and Tomasi[9] noted that even including the rotation transformation in the optimization criterion can lead to numerical instability. Following these observations, in this study translation and rotation are computed one after the other in an iterative loop. One of the most popular optimization criteria, and the one used in this paper, is the sum of the squared differences. Nevertheless, other optimization criteria are possible. For instance, Haker *et al*[10] use a Monge-Kantorovich distance that leads to a parameter free formulation. Another property of their formulation is that the optimal mapping equals the inverse mapping. This property is also found in other methods, for instance in[11]. In this study, a registration procedures derived from optimizing the sum of the squared differences is presented. The method is used to register two point sets from vector-valued functions. One-dimensional registration has been preluded in the context of projection based methods. Alliney and Morandi[12] presented a method that uses only the row and column projections of an image. They proposed to calculate the Fourier transform to compute phase correlation.

The rest of this document is organized as follows. In §2, it is described a registration procedure to compute the local properties of rotation and translation. Then, in §3, the global constraint about circularity is enforced. Next, in §4, the experimental results are shown. Finally, the document concludes.

2 Local Processing

In this section, a framework to compute the border transformation from frame to frame is introduced. First a vector-valued procedure for point set registration to

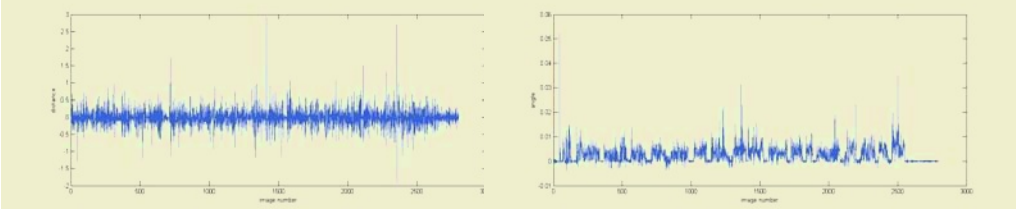

(a) Radio displacements. It is possible to appreciate abrupt changes about every 50 frames or so. This motion is due because we manually executed the gear's rotation.

(b) Angle displacements. Note the quasi-periodic bursts about every 100 frames or so.

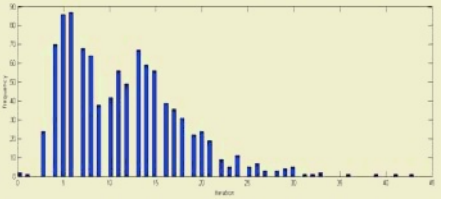

(c) Frequency of the number of iterations. In the average, the number of iterations was 11.49 with an standard deviation of 6.2548.

Fig. 3. Registration of vector-valued curve segments.

compute the translation is developed. Then a closed form equation to estimate the rotation is presented.

2.1 Translation

In [9], Shi and Tomasi introduced a procedure for region based feature tracking. In a similar way, here it is introduced a method for vector-valued point set registration. Let $\mathbf{f}(s) = [x_f(s), y_f(s)]^T$ and $\mathbf{g}(s) = [x_g(s), y_g(s)]^T$ be two vector-valued functions, the problem is to compute their best match in a short portion C of the curve S. The following similarity function is used

$$e(\delta) = \int_C \parallel \mathbf{f}(s) - \mathbf{g}(s+\delta) \parallel^2 ds \tag{1}$$

The term $e(\delta)$ is minimum when $\partial e(\delta)/\partial\delta = 0$, thus

$$\frac{\partial e(\delta)}{\partial \delta} = 2 \int_C \frac{\partial \mathbf{g}^T(s+\delta)}{\partial \delta} [\mathbf{g}(s+\delta) - \mathbf{f}(s)] ds \tag{2}$$

A possible way to express $\mathbf{g}(s+\delta)$ is by expanding it in terms of its Taylor's series and taking its linear order terms while neglecting higher order ones. Thus $\partial e(\delta)/\partial\delta$ can be approximated as

$$\frac{\partial e(\delta)}{\partial \delta} \approx 2 \int_C \mathbf{h}(s)^T (\mathbf{g}(s) + \delta \mathbf{h}(s) - \mathbf{f}(s)) ds \tag{3}$$

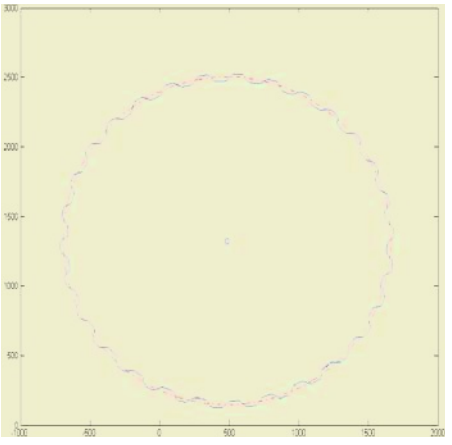

(a) As global coherence is provided local transformations are corrected. The dotted line signals the computed pitch circle. The center is in $(483.2, 1324.6)$ and the radius is 1,177.6 pixels.

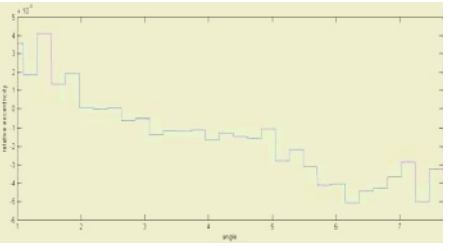

(b)Gear's eccentricity measured as the distance from the centroid to the boundary points relative to the computed radius. The values are between -5.9870×10^{-3} and 4.8334×10^{-3} relative to the radius distance.

Fig. 4. Iterative boundary measurements. In (a) the coherence constraint lead to a better fit in a global scale. In (b) this particular gear's eccentricity is presented.

where $\mathbf{h}(s) = \partial \mathbf{g}(s)/\partial s$. In the previous equation, the term δ represents the solution given the linear behavior assumption. Nonetheless, for real data, it is required to iterate until convergence is achieved. Thus δ, the relative displacement along the curve, is given by

$$\delta_{k+1} = \delta_k + \frac{\int_C \left[\mathbf{f}(s) - \mathbf{g}(s)\right]^T \mathbf{h}(s) ds}{\int_C \mathbf{h}(s)^T \mathbf{h}(s) ds} \tag{4}$$

2.2 Rotation

Here, a closed form equation to compute de angle between curve segments is derived. The transformation between a point $\mathbf{x} \in \mathbf{f}(s)$ and another point $\mathbf{y} \in \mathbf{g}(s)$ is given by

$$\mathbf{y} = R(\alpha)(\mathbf{x} - \mathbf{t}) \tag{5}$$

where $\mathbf{t}$ is the vector that makes coincide the center of rotation for both curves and $R(\alpha)$ is a 2×2 rotation matrix that depends on the angle α. A dissimilarity function relative to the different angle may be

$$\xi(\alpha) = \int_C \parallel \mathbf{y} - R(\alpha)(\mathbf{x} - \mathbf{t}) \parallel^2 ds \tag{6}$$

In order to find the minimum, $\xi(\alpha)$ is derived with respect to α. Expanding this result gives

$$\frac{\partial \xi(\alpha)}{\partial \alpha} = 2 \int_C [y_1, y_2] \begin{pmatrix} \sin\alpha \cos\alpha \\ -\cos\alpha \sin\alpha \end{pmatrix} \begin{pmatrix} x_1 - t_1 \\ x_2 - t_2 \end{pmatrix} ds \tag{7}$$

where $\mathbf{y}(s) = [y_1, y_2]^T$, $\mathbf{x}(s) = [x_1, x_2]^T$ and $\mathbf{t} = [t_1, t_2]^T$ respectively. Solving for α gives the following equation

$$\tan\alpha = -\frac{\int_C [y_1(x_2 - t_2) - y_2(x_1 - t_1)]\, ds}{\int_C [y_1(x_1 - t_1) - y_2(x_2 - t_2)]\, ds} \tag{8}$$

3 Global Correspondence

The scheme developed in the previous section is numerically error prone because the computations carry imprecisions from frame to frame. In this section, a framework for global coherence is developed. It is possible to observe that once defined a centroid and a radius, profile segments must couple smoothly as the border is processed. So we use the periodicity present in the border polar representation. Let $d(\theta)$ the function describing the objects border in polar coordinates. Then, its Fourier transform can be expressed as

$$D(f) = \sum_{k=0}^{N} d(\theta_k) e^{-2j\pi f \theta_k} \tag{9}$$

where N is the number of points in the border. Then

$$f_0 = \max_f \parallel D(f) \parallel^2 \tag{10}$$

is the frequency that describes the teeth periodicity. The number of teeth M observed is

$$M = N f_0 \tag{11}$$

Due to error propagation, the angle may have been overshot or undershot. To normalize it, the angle is multiplied by the factor

$$c = \frac{2\pi M}{T\theta_{\max}} \tag{12}$$

where T is the number of teeth in the gear and $\theta_{\max}$ is the maximum angle in the border sequence.

4 Experimental Results

A gear is placed in front of a camera (see Fig. 1). Then, the gear is rotated, manually, very slowly while grabbing 2,801 snapshots. The gear is standing on a

metallic base. This causes considerable friction. Before being used the images are corrected using Zhang[5] camera calibration procedure. The center of rotation is expected to move from frame to frame. The gear used for experimenting is spur and internal.

The border is detected using Canny's edge detector. To avoid interrupted curves the edge image is dilated using a kernel $s = \begin{pmatrix} 1 & 1 \\ 1 & 1 \end{pmatrix}$. The resulting set of points is represented by a set of line segments using a divide and conquer strategy. The line segments are in turn used to represent the vector-valued functions. In Fig. 2, it is show a typical contour image. It includes the set of profile points and the piecewise approximation with line segments. For this particular image there are 401 border points that are reduced to 48 lineal segments. In the whole sequence 1,680,600 boundary points are collected.

The initial estimation of the centroid $(\overline{x}, \overline{y})$ and radius r is computed using Nelder's simplex[13]. The translation and rotation of the vector-valued curves is computed from frame to frame. In Fig. 3, these results are presented. As it was expected, it is possible to appreciate abrupt changes about every 75 frames or so. The angular coordinates vary between about cero and 0.01 degrees. The radius changes between -0.5 and 0.5 pixels from frame to frame. In the average, the number of iterations is 11.49 with an standard deviation of 6.2548. The frame to frame registration provided a good base to compute correspondence over larger steps. The angle computation is rather good because at the end the angle missed by an offset of 4.5%. In Fig. 4(a) the reconstructed image of the gear's boundary is presented. Then, in Fig. 4(b) the estimated gear's eccentricity is presented. The eccentricity is defined as the relative variation in radial distance from the centroid. The values are between -5.9870×10^{-3} and 4.8334×10^{-3} relative to the radius distance (1,177.6 pixels). Since the model of the circle is computed over all the collected points, the circle tends to pass through the gear's pitch.

5 Conclusion

This paper presents a data-driven approach to profile fitting where global constraints are imposed to the local measurements. As the level of detail in the image increases, less reliable for tracking is the information at a particular window resolution. It is demonstrated how a combination of accurate local processing techniques with clear global constraints can negotiate with this trade-off.

As an example, an application to measure the eccentricity in internal spur gears is presented. Gears are fundamental in a myriad of mechanical devices. In the context of this study, the gears are an excellent example because they have to be measured with high precision. Thus on the one hand, they demand high resolution. On the other hand, they exhibit information useful for tracking. The proposed approach iteratively finds the geometric transformation between frames allowing, later on, to enforce global coherence.

It has been shown that the method measures the eccentricity in the border's profile. Also, the method has been shown robust against change in rotation speed, and small variations between the gear's and the camera's reference systems.

References

1. David Marr. *Vision*. W. H. Freeman, 1982.
2. Shimon Ullman. *High-Level Vision*. MIT Press, 1995.
3. Bruce A. Wilson. *Dimensioning and Tolerancing Handbook*. Genium Publishing, 1995.
4. S. J. Martin, M. A. Butler, and C. E. Land. Ferroelectric Optical Image Comparator using PLZT Thin Films. *Electronics Letters*, 24(24):1486–1487, 1988.
5. Zhengyou Zhang. A Flexible New Technique for Camera Calibration. *IEEE Transactions on Pattern Analysis and Machine Intelligence*, 22(11):1330–1334, 2000.
6. Lisa Gottesfeld Brown. A Survey of Image Registration Techniques. *ACM Computing Surveys*, 24(4):325–376, 1992.
7. Maintz and Viergever. A Survey of Medical Image Registration. *Medical Image Analysis*, 2(1), 1998.
8. F. Kruggel M. Tittgemeyer, G. Wollny. Visualising Deformation Fields Computed by Non-Linear Image Registration. *Computing and Visualization in Science*, 5(1):45–51, 2002.
9. Jianbo Shi and Carlo Tomasi. Good Features to Track. In *IEEE Conference on Computer Vision and Pattern Recognition*, pages 593–600, 1994.
10. Steve Haker, Allen Tannenbaum, and Ron Kikinis. Mass Preserving Mappings and Image Registration. *Lecture Notes in Computer Science*, 2208:120, 2001.
11. G.E. Chirstensen and H.J. Johnson. Consistent Image Registration. *IEEE Transactions on Medical Imaging*, 20(7):568 –582, July 2001.
12. S. Alliney and C. Morandi. Digital Image Registration using Projections. *IEEE Transactions on Pattern Analysis and Machine Intelligence*, 8(2):222–233, 1986.
13. William H. Press, William T. Vetterling, Saul A. Teukolsky, and Brian P. Flannery. *Numerical Recipes in C++: the Art of Scientific Computing*. Cambridge University Press, 2002.